

## Performance of Civil Aviation Receivers During Maximum Solar Activity Events

Lina Deambrogio, Christophe Macabiau, Willy Vigneau, Jean-Jacques  
Valette, Mikaël Mabillean, Emilien Robert

► **To cite this version:**

Lina Deambrogio, Christophe Macabiau, Willy Vigneau, Jean-Jacques Valette, Mikaël Mabillean, et al.. Performance of Civil Aviation Receivers During Maximum Solar Activity Events. ION PNT 2013, Pacific Positioning, Navigation and Timing Meeting, Apr 2013, Honolulu, United States. ION, pp 986-994, 2013. <hal-00937582>

**HAL Id: hal-00937582**

**<https://hal-enac.archives-ouvertes.fr/hal-00937582>**

Submitted on 3 Feb 2014

**HAL** is a multi-disciplinary open access archive for the deposit and dissemination of scientific research documents, whether they are published or not. The documents may come from teaching and research institutions in France or abroad, or from public or private research centers.

L'archive ouverte pluridisciplinaire **HAL**, est destinée au dépôt et à la diffusion de documents scientifiques de niveau recherche, publiés ou non, émanant des établissements d'enseignement et de recherche français ou étrangers, des laboratoires publics ou privés.

# Performance of Civil Aviation Receivers during Maximum Solar Activity Events

Lina DEAMBROGIO, Christophe MACABIAU, *ENAC/Université de Toulouse, Toulouse, France*

Willy VIGNEAU, *M3SYSTEMS, Toulouse, France*

Jean-Jacques VALETTE, *CLS, Toulouse, France*

Mikael MABILLEAU, *Egis Avia, Toulouse, France*

Emilien ROBERT, *EUROCONTROL, Bruxelles, Belgium*

## BIOGRAPHIES

**Lina DEAMBROGIO** received the Master degree in Telecommunication Engineering in 2007 and the PhD in 2012 both from the University of Bologna, Italy. From March 2012 she is a researcher in the signal processing lab of ENAC in Toulouse, France. Her research focuses on the study of signal processing techniques for GNSS receivers in degraded scenarios.

**Christophe MACABIAU** graduated as an electronics engineer in 1992 from the ENAC in Toulouse, France. Since 1994, he has been working on the application of satellite navigation techniques to civil aviation. He received his PhD in 1997 and has been in charge of the signal processing lab of ENAC from 2000 to 2012. He is currently the head of the TELECOM lab of ENAC.

**Willy VIGNEAU** is head of the Radionavigation Unit at M3 Systems. Graduated as a Telecommunication Engineer from SUPAERO (Ecole Nationale Supérieure de l'Aéronautique et de l'Espace), he joined M3 Systems in 1999, a French SME (Toulouse) involved in various Radionavigation projects: GPS/EGNOS/Galileo signal processing and critical applications of satellite Radionavigation.

**Jean-Jacques VALETTE** obtained a PhD thesis in 1992 at Groupe de Recherche de Géodésie Spatiale, University Paul Sabatier of Toulouse, on Geophysics and Space Technics. He has been working at CLS as an engineer in the Metrology of Space Systems Departement and since 2009 in the System and Radio-Frequency Engineering Department. He has been involved in space geodesy for high precision ground positioning projects or the Earth Reference System (DORIS, GNSS). He has been responsible for various space weather studies since 2003 on the fields of ionosphere scintillations, solar energetic particles and on the implementation of operational services.

**Mikael MABILLEAU** graduated from ENAC (French Civil Aviation School) in August 2006 and has integrated

Egis Avia as CNS project Engineer. He has been involved since 2006 in Galileo standardization activities for Civil Aviation in the frame of the EUROCAE WG 62 and ICAO NSP group. He is also involved in new concept of operation and new system definition through its work on Advanced RAIM and SBAS L1L5 proposition of standard. Since 2009, Mikael has been contributing in an ionosphere study with the objective to assess the impact of ionosphere perturbation on civil aviation applications using GNSS during the upcoming period of high solar activity.

**Emilien ROBERT** got his PhD in 2005 and started to work on behalf of Airbus as a Flight Management Engineer. The Flight Management System is the main navigation computer on board aircraft. In 2007, he worked on behalf of ATR as a Navigation Engineer and broadened his experience in the field of Navigation equipment and sensors. These two work experiences gave him a strong background on Navigation as well as on avionics and on board equipment. Emilien joined Eurocontrol in 2010 as a Navigation expert and since then, is in charge of a project assessing the space weather impact on GNSS based operation.

## ABSTRACT

Nowadays, Global Navigation Satellite Systems (GNSS) are widely employed in all aircraft operations from en-route to approach and landing. However, relying on the reception of satellite signals to compute the user position, GNSS receivers must take into account all possible perturbations caused by propagation through the ionosphere that might affect and degrade the signals.

In nominal conditions, the only ionospheric effect on GNSS signals is the introduction of an additional group delay and phase advance caused by a change in group and phase propagation velocity proportional to the ionospheric Total Electron Content (TEC) along the signal path and the signal frequency. However, during high solar activity periods, other abnormal behaviors can occur. For example, occasionally small-scale irregularities in the electron density can appear causing the scattering of impinging satellite signals in multiple paths that are later summed coherently at the receiver, generating deep power

fades and rapid changes in the signal phase. Moreover, solar burst events could also take place, leading to wide-band interference and to a strong degradation of quality of received signal processing.

Since civil aviation operations will be increasingly dependent on the use of GNSS in Europe for navigation or surveillance purposes, it is imperative to understand the impact of the ionosphere on GNSS based applications during different phases of flight and to develop and validate mitigation techniques to ensure and maintain the safety and performance requirements for aviation operations.

In this context, the EUROCONTROL (European Organization for the Safety of Air Navigation) project “Effects of solar activity over ECAC”, has indeed the aim to assess the potential effect of solar activity (scintillation and ionospheric gradients) over the ECAC region and to identify mitigation techniques applying ionospheric models to aviation applications.

Within the framework of the EUROCONTROL project, the focus of this paper is to evaluate the robustness of the different civil aviation GNSS receivers signal processing blocks to ionospheric disturbances by modeling efficiently the effect of ionosphere activity on the behavior of an aeronautical receiver.

## INTRODUCTION

The impact of the nominal and anomalous ionosphere behavior on GNSS signal propagation have already been investigated in the past yielding to the definition of different models (e.g. Klobuchar [1], NeQuick [2], Cornell Scintillation Model [3]) and the evaluation of receiver performance [4]. However, a thorough evaluation of ionospheric effects on the civil aviation receiver signal processing blocks during a period of high solar activity in Europe has not yet been carried out. Nevertheless, with the approach of the next solar peak in 2013 this characterization has become necessary.

Signal processing is in fact the first stage in the receiver that is impacted by ionospheric-induced errors and that may need to be enhanced to improve tracking loop robustness to signal fluctuations in periods of intense solar activity. Besides signal processing, position level mitigation and integrity monitoring could also need to be considered as a further step to be evaluated.

In order to assess the robustness of the receivers and the impact of the ionosphere on the signal processing blocks, the following steps are detailed in the paper: the description of the list of ionospheric events and the evaluation of the receiver performance. More in detail, the evaluated events are defined within the framework of the EUROCONTROL project named “Effects of solar activity over ECAC” considering nominal and worst case events (large TEC variations and/or scintillations) as reported in literature.

This paper further details the simulator used for the testing. It has been designed to model each civil aviation GNSS receiver characteristic following their definitions in

standards such as the ICAO Annex 10, RTCA and EUROCAE. Moreover, since for civil aviation operations the core satellite constellations need to be augmented, all three types of augmentation defined at ICAO level (ABAS, SBAS and GBAS) have been considered. The aim of the simulator is to represent each receiver and error. Indeed, the simulator uses as the input component a complete model of the correlator outputs, thus providing a “behavioural” simulation of the signal processing stage. All effects including the anomalous ionospheric perturbations are used to shape the impact of received signal parameters on the correlator outputs. This way, the effect of dynamics, local oscillator, ionospheric delay and scintillation, are all used to compute the incoming signal code delay and carrier phase and Doppler.

The paper also presents simulation results that quantify the receiver performance degradation in terms of code, phase, Doppler tracking errors, cycle slips and loss of lock. These results will provide a preliminary analysis and guidance material to develop a model of the ionosphere impact on aeronautical receivers over the ECAC. This initiative extends studies previously started in different European countries and it allows the development of a genuine ionosphere impact model suitable for aviation operational needs.

## I. IONOSPHERIC EVENTS

The ionosphere is the layer in the upper atmosphere characterized by the presence of free electrons and ions produced by solar emissions. The free electrons affect the propagating signals with frequency dependent behaviors that range from the introduction of delays to rapid variations in the signal amplitude and phase [5]. It must be noted that the behavior of the ionosphere, regarding its observable effects on radio signals, varies with solar activity, time and location. Moreover, the solar activity changes with the season, the time of day and the 11-year solar cycle.

In nominal conditions, the presence of free electrons in the ionosphere affects the velocity of the propagating waves, resulting in a time delay of the GNSS signal code and an advance of the carrier equal to [6]:

$$\Delta S = \frac{40.3}{f^2} \int_{SV}^{User} n_e dl \quad (1)$$

Where  $\Delta S$  is the delay/advance introduced by the ionosphere in seconds and  $TEC = \int_{SV}^{User} n_e dl$  is the Total Electron Content (TEC), which is related to the electron density ( $n_e$ ) along the path connecting receiver and satellite.

## II. TEC GRADIENTS

The nominal TEC content undergoes daily variations and can differ from one region to the other due to the

inclination of the sun rays. These TEC differences between regions generate gradients that may affect crossing signals with different ionospheric delays compared to the case of a signal propagating through a homogeneously ionized layer. This is especially true in equatorial regions while at mid-latitudes, TEC normally shows a smooth spatial variation [7]. In the presence of Travelling Ionospheric Disturbances (TID), perturbations might also generate temporal and spatial TEC gradients that are not accounted for in models such as Klobuchar [1] and NeQuick [2], which are representative of nominal space weather conditions only. This time and space-dependent changes in the electron density content could pose problems to tracking loops if the rate of change is too fast for the loops to follow. Since the focus of this work is on characterizing the response of the signal processing block, only temporal gradients will be taken into consideration in the following.

### III. SCINTILLATIONS

In high solar activity periods, disturbances and irregularities may also originate within the ionosphere causing rapid fluctuations in the received signals. Indeed, the presence of anomalies in the refraction index can cause the signals to scatter in random directions inducing amplitude and phase scintillations. At the receiver, the combination of the scattered signal paths produces amplitude scintillations, which consist in both deep signal fades and shallow enhancements, and phase scintillations that are observed as rapid fluctuations in the carrier phase shift [8] [9].

The received GNSS signal affected by scintillation can therefore be modeled as:

$$r(t) = A_0 \delta A c(t - \tau) d(t - \tau) \cos(2\pi f_0 t - \theta - \delta\varphi) + n(t) \quad (2)$$

Where:

- $A_0$  is the nominal amplitude of the received signal
- $f_0$  is the nominal carrier frequency
- $d(t)$  is the waveform encoding the navigation message
- $c(t)$  is the waveform encoding the PRN code
- $\tau$  is the propagation delay
- $\theta$  is the received carrier phase delay due to nominal propagation
- $\delta A$  is the scintillation amplitude
- $\delta\varphi$  is the scintillation phase
- $n(t)$  is the additive white noise

Scintillations can be described through probability distributions. The fluctuations in the signal intensity are generally modeled as following a Nakagami- $m$  distribution with mean value 1 and variance  $1/m$  [6]:

$$p(I) = \frac{m^m \delta I^m}{\Gamma(m)} e^{-m\delta I} \quad (3)$$

Where  $I = A^2 = [A_0 \delta A]^2$  and  $\delta I \geq 0$ .

The effects of amplitude scintillations are characterized by the  $S_4$  index that is the normalized standard deviation of the fluctuating received signal power:

$$S_4 = \sqrt{\frac{1}{m}} = \frac{\sqrt{\text{Var}(I)}}{E[I]} \quad (4)$$

Due to properties of Nakagami distributions the constraint  $S_4 \leq \sqrt{2}$  is introduced.

Phase scintillations follow a zero mean Gaussian distribution characterized by the standard deviation  $\sigma_\varphi$ :

$$p(\delta\varphi) = \frac{1}{\sqrt{2\pi}\sigma_\varphi} e^{-\frac{\delta\varphi^2}{2\sigma_\varphi^2}} \quad (5)$$

Amplitude and phase scintillations are both highly correlated over short intervals.

Moreover, it should be noted that scintillation affects signals in different bands differently and the scintillation parameters follow the trends [6]:

$$S_4 \propto \frac{1}{f^{1.5}} \quad \text{and} \quad \sigma_\varphi \propto \frac{1}{f}$$

Finally, it should be pointed out that due to the irregular nature of the disturbances in the ionosphere, not all satellites in view may be affected by scintillations at the same time.

### IV. SCINTILLATION MODEL

In literature, different models have been defined for scintillation prediction. However, a unique scintillation generator for all latitude scintillations does not exist.

A number of scintillation generators have been developed for modeling equatorial scintillations: the Cornell Scintillation Model (CSM) [3] [9], the Global Ionospheric Scintillation Model (GISM) [10] and the Wide Band Model (WBMOD) [10] are just a few.

Nevertheless, these scintillation generators are tailored specifically to equatorial regions and built upon a large collection of scintillation observations carried out in low latitude regions only.

Differently from the equatorial case, in Polar Regions, scintillations are characterized by low amplitude scintillations and strong phase scintillations [8] [11] that cannot be synthesized with the previously mentioned generators. This is why in the following, in order to use a unique scintillation model for all latitudes, scintillation is

generated as described in [11] and [12]. The scintillation amplitude is assumed as following a Gamma distribution that approximates the Nakagami-m distribution:

$$p(I) = \frac{\left(\frac{I}{\beta}\right)^{\alpha-1}}{\beta\Gamma(\alpha)} e^{-I/\beta} \quad (6)$$

with  $\alpha = 1/\beta = 1/S_4^2$ .

The phase scintillations are modeled as following the Gaussian distribution defined in Equation (5).

Since the amplitude and phase scintillations are in this case generated independently, no canonical fades are simulated. Furthermore, it is important to note that no time correlation has been implemented between the samples making it a worst case scenario for signal processing.

## V. SCENARIO DEFINITION

This section presents the scenarios identified to perform the characterization of the impact of the ionosphere on aeronautical receivers and civil aviation operations.

The scenarios have been selected to represent different potential behaviours of the ionosphere over the ECAC area. Since a statistical approach could not be developed due to the lack of a relevant database, the scenario parameters are herein taken from bibliography and observed ionospheric behaviour. It should be noted that this limitation should be overcome in the coming years thanks to the on-going EUROCONTROL IONO project activities.

In this work only single channel signal tracking performance are studied, thus the analysis is carried out considering one received signal affected by ionospheric induced errors.

In order to characterize the effect of a TEC gradient, a simplified model, where only the temporal gradient is considered, is applied. Thus, in this model, the additional delay to the received signal increases linearly with time until it reaches the maximum.

TEC Settings:

- **Max delay value:** Maximum delay value reachable during the scenario [13];
- **Temporal Gradient:** Evolution of the VTEC according to the time [14].

The scintillation values for the polar region were taken from [11] selecting as the nominal case the weak scintillation values and as worst case the strong scintillation values. The Equatorial Region scintillation parameters are taken from [13].

Scintillation Settings:

- **S4 level:** Level of S4 representing the amplitude scintillation;
- **$\sigma_\phi$  level:** Level of  $\sigma_\phi$  representing the phase scintillation.

The selected scenarios are summarized in Table 1:

Parameter	Sub-parameter	Global Scenario	Worst Global Scenario	Polar Region	Worst Polar Region	Equatorial Region	Worst Equatorial Region
TEC	MAX VTEC	30 m	50 m	30 m	50 m	30 m	50 m
	VTEC temporal gradient	30 mm/s	150 mm/s	30 mm/s	150 mm/s	30 mm/s	150 mm/s
Scintillation	S <sub>4</sub>	-	-	0.06 [11]	0.06 [11]	0.5 [13]	1 [13]
	$\sigma_\phi$	-	-	0.2 rad [11]	0.6 rad [11]	0.5 rad [13]	1 rad [13]

Table 1 Ionospheric scenario definition

## VI. AVIATION RECEIVER MODELS

Different types of civil aviation GNSS receivers have been considered in this study. Their characteristics follow the definitions in standards such as the ICAO Annex 10, RTCA and EUROCAE. It must be noted that for civil aviation operations the core satellite constellations need to be augmented, this is why all three types of augmentation defined at ICAO level (ABAS, SBAS and GBAS) have been considered.

The receivers considered in the study are:

- ABAS basic receiver (old TSO C 129 – DO 208)
- ABAS TSO C 196 receiver (DO 316)
- GBAS (GAST C) airborne receiver (DO 253-C)
- SBAS airborne receiver (GPS signal processing)

Only the airborne GBAS receiver is considered given that the worst scenario is assumed to be when the ionosphere anomaly affects only the airborne receiver and it is not observable from the ground station.

Furthermore, given that the signal processing block of the airborne SBAS receiver with GPS signal processing is equal to the GBAS, it will not be tested separately.

The receivers' tracking block characteristics are reported in Table 2.

For all considered receivers, the PLL discriminator implemented is a two-quadrant arctangent (ATAN) while the DLL discriminator is the non-coherent early minus late power (EMLP).

	RF/IF Filter Bandwidth	PLL Discriminator	BPLL	DLL Discriminator	BDLL	Chip spacing
ABAS TSO C 129 (DO 208)	2 MHz	ATAN	10 Hz	EMLP	1 Hz	1
ABAS TSO C 196 receiver (DO 316)	20 MHz	ATAN	10 Hz	EMLP	1 Hz	0.1
GBAS GAST C airborne receiver (DO 253 C)	10 MHz	ATAN	10 Hz	EMLP	1 Hz	0.1

Table 2 Receiver characteristics

## VII. SIMULATION SET-UP

The aim of the simulator is to represent each receiver tracking block and output their estimated errors. Indeed, the simulator uses as the input component a complete model of the correlator outputs, thus providing a behavioral simulation of the signal processing stage. All effects including the anomalous ionospheric perturbations are used to shape the impact of received signal parameters on the correlator outputs. This way, the effect of dynamics, local oscillator, ionospheric delay and scintillation, are all used to compute the incoming signal code delay and carrier phase and Doppler.

It must be noted that the anomalous ionospheric components that will be analyzed with this simulator will be reflected with a time step of 20ms. However, based on characteristics of ionospheric anomalies provided in publications, 50Hz seem sufficient to model the impact of possible ionospheric events.

This simulator will thus model the behaviour of the signal processing algorithms (i.e. the tracking loops) at the output of the correlators process and assess the re-acquisition when the tracking is lost.

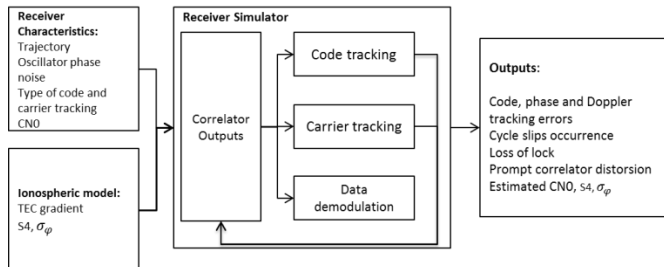


Figure 1 Simulation Environment

The simulated receiver dynamics are characterized by a constant jerk dynamic where a succession of negative jerk pulses lasting 3s is followed by positive jerk pulses lasting 6s. This way, the receiver velocity and acceleration change with time while remaining bounded also for long simulation tests.

The validity of this model to reflect civil aviation receivers has been checked for several aspects in previous projects and is herein used to test the robustness of civil aviation receivers during periods of high solar activities.

## VIII. NUMERICAL RESULTS

The receiver characteristics are reported in Table 2, the common features include a Brickwall RF/IF filter and a Temperature Compensated Crystal Oscillator (TCXO) with parameters:  $h_0 = 1e-21$ ,  $h_1 = 1e-20$  and  $h_2 = 2e-20$ .

At the start of the simulations the receiver is considered locked and in initialization phase. This initialization phase lasts 360s and it is used to allow the smoothing filter to converge. After initialization, the scintillation and TEC effects are included in the simulation. The simulations have considered two different ionospheric threat models:

- TEC gradient scenarios (temporal rate associated to different iono events)
- Scintillation scenarios (Variation of  $S_4$ ,  $C/N_0$  and  $\sigma_\varphi$  associated to different iono events)

The results reported in this section characterize the civil aviation receiver performance in the identified scenarios and can be used as a guideline for employing these receivers in the presence of high solar activity events.

Results quantify the receiver performance degradation in terms of code, phase, Doppler tracking errors, cycle slips and carrier phase lock availability. The tracking error performance is computed considering one run simulations of 1720s (in order to accommodate an initial and final 360s smoothing filter convergence interval and an additional 1000s to allow also the nominal TEC gradient to reach its maximum). Moreover, since in civil aviation operations the PLL needs to be locked, statistics are computed considering only the points in the simulation that have PLL lock. Furthermore, the percentage of PLL lock is computed from the start of the ionospheric disturbance.

The results are grouped by Global Scenarios (nominal and worst cases), Polar Region (nominal and worst cases) and finally Equatorial Region (nominal and worst cases). For each scenario two different  $C/N_0$  values have been tested. In the Global scenario, the only ionospheric effect considered is the presence of TEC temporal gradients following the characteristics defined in Table 1.

Receiver type	Severity of Iono event	CN0 (dB Hz)	Std of phase error (rad)	Std frequency error (Hz)	Std uns mooth code error (m)	Std smoooth code error (m)	cycl e slips	% PLL availability
ABAS basic receiver	Nominal case	35	0.19	0.72	3.52	0.14	0	100
	max VTEC=30m gradien t=30 mm/s	40	0.18	0.67	1.94	0.06	0	100
	Worst case	35	0.19	0.73	3.42	0.14	0	100
	max VTEC=50m and gradien t=150 mm/s	40	0.18	0.67	1.95	0.06	0	100
ABAS TSO C 196	Nominal case	35	0.19	0.72	1.06	0.05	0	100
	max VTEC=30m gradien t=30 mm/s	40	0.18	0.66	0.58	0.03	0	100
	Worst case	35	0.19	0.72	1.03	0.05	0	100
	max VTEC=50m and gradien t=150 mm/s	40	0.18	0.66	0.58	0.03	0	100
GBAS	Nominal case	35	0.19	0.72	1.14	0.06	0	100
	max VTEC=30m gradien t=30 mm/s	40	0.18	0.66	0.63	0.03	0	100
	Worst case	35	0.19	0.72	1.12	0.06	0	100
	max VTEC=50m and gradien t=150 mm/s	40	0.18	0.66	0.63	0.03	0	100

**Table 3 Global Scenario receiver performance with TEC gradients and no scintillation**

As shown from the results in Table 3, the identified TEC temporal gradients do not pose particular problems to the tracking loops that are able to follow the changes without losing lock.

Phase tracking performance is influenced in this scenario by receiver dynamics, local oscillator and noise, yielding a standard deviation of 0.19 rad and 0.18 rad at 35 dBHz and 40 dBHz respectively. On the other hand, code tracking performance is steered by receiver dynamics, noise, chip space setting and the TEC gradient. The difference in the results' accuracy regarding the code tracking block are ascribable to the different chip space settings of the receivers.

With Polar and Equatorial Regions, also scintillation effects must be considered. In these scenarios the ability of the tracking loops, and especially the PLL to follow the changes in the received signal are severely tested.

Receiver type	Severity of Iono event	CNO (dB Hz)	Std of phase error (rad)	Std frequency error (Hz)	Std uns mooth code error (m)	Std smoooth code error (m)	cycl e slips	% PLL availability
ABAS basic receiver	Nominal case	35	0.26	0.86	3.5	0.13	0	100
	TEC gradient	40	0.25	0.82	2	0.06	0	100
	Worst case	35	N/A	N/A	N/A	N/A	N/A	0
	TEC gradient	40	N/A	N/A	N/A	N/A	N/A	0
	S4=0.06	35	0.25	0.85	1.0	0.05	0	100
	$\sigma_{\varphi}=0.2$ rad	40	0.25	0.81	0.6	0.02	0	100
ABAS TSO C 196	Nominal case	35	0.25	0.85	1.0	0.05	0	100
	TEC gradient	40	0.25	0.81	0.6	0.02	0	100
	Worst case	35	N/A	N/A	N/A	N/A	N/A	0

	S <sub>4</sub> = 0.06 σ <sub>φ</sub> = 0.6 rad							
		40	N/A	N/A	N/A	N/A	N/A	0
GBAS	Nominal case TEC gradient	35	0.26	0.84	1.14	0.05	0	100
	S <sub>4</sub> = 0.06 σ <sub>φ</sub> = 0.2 rad	40	0.26	0.81	0.6	0.02	0	100
	Worst case TEC gradient	35	N/A	N/A	N/A	N/A	N/A	0
	S <sub>4</sub> = 0.06 σ <sub>φ</sub> = 0.6 rad	40	N/A	N/A	N/A	N/A	N/A	0

**Table 4 Polar Region receiver performance with TEC gradients and scintillation**

In the Polar Region, the presence of ionospheric scintillations can cause difficulties to the tracking loops, the PLL in particular, as shown in Table 4. More in detail, in the nominal scintillation case, tracking is feasible 100% of the time while, similarly to [11], with amplitude scintillations equal to  $S_4=0.06$  and phase scintillations of  $\sigma_\phi=0.6$  rad, the receiver loses lock and is not able to have continuous tracking after re-acquisition.

Tracking in fact is feasible when the total phase jitter is below the tracking threshold:

$$3\sigma_{PLL} \leq \pi/2 \quad (7)$$

with  $\sigma_{PLL}$  representing the phase jitter due to all sources. The value  $\sigma_\phi=0.6$  rad can be thus considered as a critical value for PLL tracking and can be used as a threshold of tracking feasibility in the presence of scintillation.

Differently from the Global Scenario case, PLL performance in the presence of scintillation is influenced by receiver dynamics, local oscillator, thermal noise and scintillations, whose effect is an increase in the noise floor and an added term to the total phase jitter [4], obtaining an average standard deviation for the PLL equal to 0.26 rad. DLL performance is equivalent to the Global Scenario case, as the increase in noise due to amplitude scintillation is not relevant.

Differently from Polar Region scintillations, in the Equatorial Regions, scintillation is characterized both by amplitude and phase scintillations. In the scope of this project we have considered two cases as defined in Table 1, the nominal and worst scintillations cases.

The obtained performance is reported in Table 5.

Receiver type	Severity of Ionospheric event	CNO (dB Hz)	Std of phase error (rad)	Std frequency error (Hz)	Std unsmoothed code error (m)	Std smoothed code error (m)	cycle slips	% PLL availability
ABAS basic receiver	Nominal case TEC gradient	35	0.3	0.9	3.5	0.2	2	1.2
	S <sub>4</sub> = 0.5 σ <sub>φ</sub> = 0.5 rad	40	0.3	0.9	2.8	0.6	6	4.5
	Worst case TEC gradient	35	N/A	N/A	N/A	N/A	N/A	0
	S <sub>4</sub> = 1 σ <sub>φ</sub> = 1 rad	40	N/A	N/A	N/A	N/A	N/A	0
ABAS TSO C 196	Nominal case TEC gradient	35	0.2	0.8	1	0.05	2	1.1
	S <sub>4</sub> = 0.5 σ <sub>φ</sub> = 0.5 rad	40	0.2	0.8	0.6	0.02	4	1.1
	Worst case TEC gradient	35	N/A	N/A	N/A	N/A	N/A	0
	S <sub>4</sub> = 1 σ <sub>φ</sub> = 1 rad	40	N/A	N/A	N/A	N/A	N/A	0
GBAS	Nominal case TEC gradient	35	0.2	0.8	1.1	0.05	4	0.5
	S <sub>4</sub> = 0.5 σ <sub>φ</sub> = 0.5 rad	40	0.2	0.8	0.6	0.02	4	1.1
	Worst case TEC gradient	35	N/A	N/A	N/A	N/A	N/A	0



S <sub>4</sub> =								
1	40	N/A	N/A	N/A	N/A	N/A	N/A	0
σ <sub>φ</sub> =								
1								
rad								

**Table 5 Equatorial Region receiver performance with TEC gradients and scintillation**

The scintillation realization employed in the tests shows that also for the nominal condition case identified by  $S_4=0.5$  and of  $\sigma_\phi=0.5$  rad the carrier tracking loop has difficulty in following the received signal. The percentage of PLL lock in this case is quite low, causing the statistics to be incomplete as only few points are used in the computations. The unavailability of the PLL solution determines also the impossibility of having the smoothed solution. Nevertheless, these results show that in the Equatorial Region both amplitude and phase scintillation parameters must be considered to find threshold values for correct receiver operation.

In the following, as an example, the behavior of the tracking errors are reported for the ABAS TSO C 196 receiver in the presence of the nominal equatorial scintillation case and nominal C/N0=35dBHz. After the initialization phase of 360s, both TEC gradient and scintillation start acting causing the drop in estimated C/N0 as reported in Figure 2 and the loss of tracking lock depicted in Figure 3 and Figure 4.

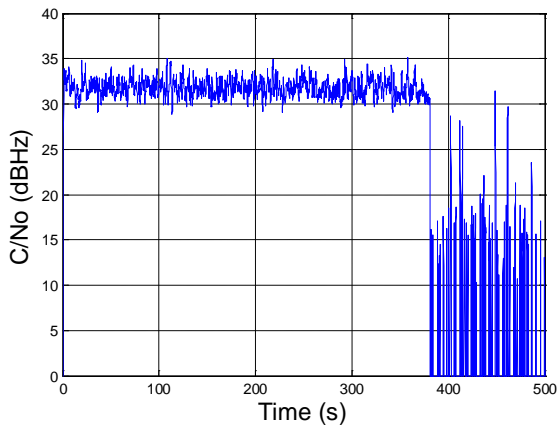


**Figure 2 Estimated C/N0 in the presence of nominal equatorial scintillations**

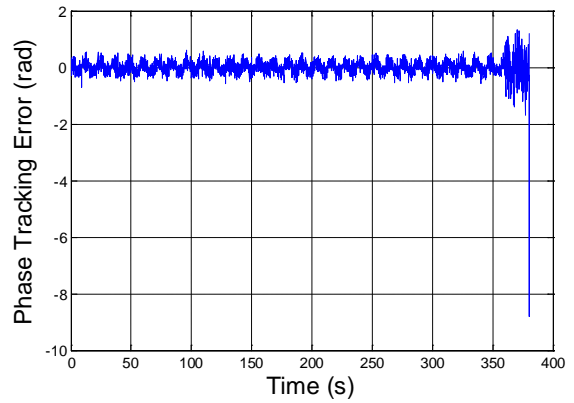


**Figure 3 Carrier phase tracking error in the presence of nominal equatorial scintillations for the ABAS TSO C 196 receiver**

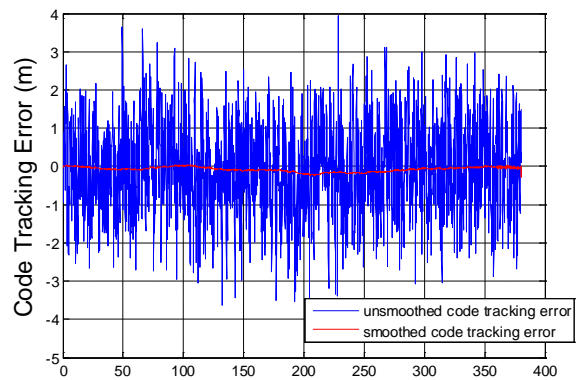


**Figure 4 Unsmoothed and smoothed code tracking error in the presence of nominal equatorial scintillations for the ABAS TSO C 196 receiver**

## CONCLUSIONS

In this paper the problem of assessing the robustness of civil aviation receivers during high solar activity events is tackled. The aim of this work is to carry out systematic tests of civil aviation receivers in defined ionospheric scenarios to provide a preliminary analysis and guidance material to develop a model of the ionosphere impact on aeronautical receivers over the ECAC.

Simulations show that the identified TEC gradients do not pose problems to the tracking loops that are able to follow the changes maintaining continuous lock with the received signal. The tested receivers have all similar phase tracking performance while the ABAS TSO C 196 and GBAS GAST C have improved code tracking performance due to their chip spacing settings.

On the other hand the presence of ionospheric scintillations can be challenging to tracking loops and in particular to PLL circuits. In this context, polar and equatorial scintillation have been considered. In the Polar Region the scintillation is characterized by feeble

amplitude scintillations and strong phase scintillations, with phase scintillation being the trigger to the loss of lock of the PLL. In particular for the identified nominal conditions of  $S4= 0.06$  and  $\sigma_\varphi= 0.2$  rad the tracking is guaranteed 100% of the time. On the other hand, in the worst case  $S4= 0.06$  and  $\sigma_\varphi=0.6$  rad, phase tracking is never achieved and therefore  $\sigma_\varphi=0.6$  rad has been identified as a tracking threshold.

Conversely, in the Equatorial Region, it is the combination of amplitude and phase scintillations that might cause the carrier phase loop to lose lock. While in the identified nominal conditions lock is not continuative and can be guaranteed only on average the 1% of the time, in the worst case, lock is never achieved.

Thanks to the studies started in different European countries on ionosphere modeling and the measurement campaigns on scintillation events over ECAC, the definition of specific scenarios for this region will allow to carry out more tailored analysis and give a more precise characterization of the civil aviation performance during high solar activity events.

## ACKNOWLEDGMENTS

The activities developed to achieve the results presented in this paper, were created by EUROCONTROL for the SESAR Joint Undertaking within the frame of the SESAR Programme co-financed by the EU and EUROCONTROL. The opinions expressed herein reflect the authors view only. The SESAR Joint Undertaking is not liable for the use of any of the information included herein."

## REFERENCES

- [1] J. Klobuchar, "Ionospheric effects on GPS", Global Positioning Systems: Theory and Applications-Volume I, volume 163, Progress in Astronautics and Aeronautics, 1996.
- [2] S. M. Radicella, "The NeQuick model genesis, uses and evolution", Annals of Geophysics, Vol 52, 2009.
- [3] Humphreys, T., M. L. Psiaki, J. C. Hinks, B. O'Hanlon, and P. M. Kintner Jr., "Simulating Ionosphere-Induced Scintillation for Testing GPS Receiver Phase Tracking Loops", IEEE Journal of Selected Topics in Signal Processing, Volume 3, Number 4, August 2009.
- [4] R. S. Conker, M. B. El-Arini, C. Hegarty, C.J. and Hsiao, T., "Modelling the Effects of Ionospheric Scintillation on GPS/Satellite-Based Augmentation System Availability". Radio Sci., 37, 1, 1001, doi: 10.1029/2000RS002604, 2003.
- [5] B. W. Parkinson and J. J. Spilker, "Global Positioning Systems: Theory and Applications-Volume I", volume 163, Progress in Astronautics and Aeronautics, 1996.

[6] E. D. Kaplan, C. Hegarty, "Understanding GPS: Principles and Applications," Artech House Mobile Communications Series, 2006.

[7] A. DasGupta, A. Paul, A. Das, "Ionospheric total electron content (TEC) studies with GPS in the equatorial region", Indian Journal of Radio & Space Physics Vol. 36, August 2007, pp. 278-292.

[8] "Effect of Ionospheric Scintillations on GNSS – A White Paper", SBAS Ionospheric Working Group (Stanford University), November 2010.

[9] P. Kintner, T. Humphreys, J. Hinks, "GNSS and Ionospheric Scintillation: How to Survive the Next Solar Maximum", InsideGNSS July-August 2009.

[10] CIGALA Project State of the art review D2.1-WP200 V1. FINAL VERSION. 7th Framework Program Grant Agreement No:247920.

[11] F. Ghafoori and S. Skone, "High Latitude Scintillation Analysis for Marine and Aviation Applications", ION GNSS 2012, Session A5.

[12] C. Hegarty, M. B. El-Arini, T. Kim, S. Ericson, "Scintillation modelling for GPS – Wide Area Augmentation System receivers", Radio Science, Vol. 36, N. 5, Sept-Oct. 2001.

[13] D2.2 Final Work Plan of EUROCONTROL funded "Study on the Impact of Solar Activities on Aviation Applications Based on GNSS over ECAC", CONTRACT N° C2357.

[14] S. Datta-Barua, "Ionospheric Threats to Space-Based Augmentation System Development", Proc. Of ION GNSS 2004, Long Beach, CA, Sept. 21\_24, 2004.